Seismic Response and Design Implications of Single-Storey Steel Cantilever Structures: Evidence from the 2023 Kahramanmaraş Earthquake

Tzvetan Georgiev

Dept. "Steel, Timber and Plastic Structures", University of Architecture, Civil Engineering and Geodesy, 1 H. Smirnenski Blvd., Sofia 1046, Bulgaria

*Corresponding author: **cvgeorgiev_fce@uacg.bg**

https://doi.org/10.5755/j01.sace.44419

JSACE 2/40

Seismic Response and Design Implications of Single-Storey Steel Cantilever Structures: Evidence from the 2023 Kahramanmaraş Earthquake

Received 2026/03/06

Accepted after revision 2026/05/21

Abstract

The 2023 Kahramanmaraş earthquake sequence in Türkiye generated ground motions that locally exceeded the design seismic action prescribed by national codes, highlighting uncertainties regarding the seismic reliability of different structural systems. While multi-storey steel frames are extensively addressed in seismic design standards, significantly less attention has been devoted to single-storey cantilever steel structures, where plasticity is typically concentrated at column bases and structural redundancy is limited.

This study investigates the seismic response of a single-storey steel cantilever structure located in Antakya, which survived the earthquake without collapse despite experiencing high seismic demand. The research combines field observations, modal analysis, response spectrum analysis (RSA), and nonlinear dynamic analyses (DNA) using recorded strong motion accelerograms from nearby seismic stations. Modelling assumptions, input motions, and performance criteria are explicitly defined to ensure methodological transparency.

The results indicate that the observed structural survival can be attributed to controlled plastic hinging at the column bases, adequate restraint against column instability, and limited but stable energy dissipation capacity. Nonlinear analyses demonstrate a reduction of effective seismic demand by approximately 2.8 times compared to the elastic response, while second-order effects were shown to be non-negligible.

Based on the analytical findings, rational behaviour factor q and displacement factor q_d are proposed for the design of steel cantilever systems within the framework of Eurocode 8. The study contributes to the understanding of the seismic performance of these systems and provides design implications relevant to seismic-resistant structural engineering practice in regions of high seismic hazard.

Keywords: nonlinear dynamic analysis; seismic performance; single-storey steel structures; steel cantilever systems.

Introduction

Moment-resisting frames (MRFs) and concentrically or eccentrically braced frames (CBFs and EBFs) are the conventional structural systems used for seismic-resistant steel buildings. Their well-established advantages in multi-storey construction come from their ability to develop ductile response mechanisms and dissipate seismic energy through controlled inelastic behaviour. In regions of high seismic hazard such as Bulgaria, the Balkan region, Southeast Europe, and Türkiye, seismic action often governs the design of multi-storey steel structures. Achieving reliable ductile performance requires the consistent application of capacity design principles, strength hierarchy among members, joints and connections, and iterative detailing

ktu 1922

Journal of Sustainable Architecture and Civil Engineering
Vol. 2 / No. 40 / 2026
pp. 99-118
DOI 10.5755/J01.SACE.44419

to ensure a desirable global plastic mechanism. These measures increase design complexity, but they enable behaviour factors q in the range of 4–6 according to Eurocode 8 (CEN, 2004).

In contrast, steel structures are frequently employed in single-storey lightweight buildings requiring large unobstructed spaces, such as car showrooms, supermarkets, airport or railway reception halls, industrial facilities, and warehouses (Figs. 1, 2). These buildings are typically characterized by low self-weight due to modern lightweight roof and façade systems. The large spans between supports and the architectural demand for open interiors often make traditional MRF and CBF systems less efficient or uneconomical. One structural solution frequently adopted in practice is the steel cantilever system.

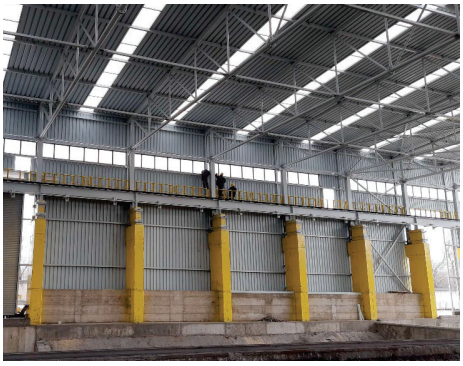
In steel cantilever systems, lateral stiffness is provided solely by the columns, which are fixed at their base and pinned at their top to the roof structure. Horizontal loads are resisted through cantilever action. The roof may consist of planar trusses, I-shaped beams, or spatial roof truss systems (Fig. 2). Column spacings typically range from 6 to 18 m, depending on functional and architectural requirements. In planar systems, columns act as cantilevers in one principal direction and are braced in the orthogonal direction by concentrically braced frames (CBFs). This arrangement is often used when structural grid spacings differ significantly between the two axes. In spatial systems, columns act as cantilevers in both principal directions, and grid spacings are comparable in plan (Fig. 2).

Fig. 1

Examples of single-storey steel buildings utilizing cantilever structural systems



a) Car showroom, Antakya, Hatay Province, photo taken by the author three months after the 6 February 2023 earthquake sequence



b) Storage facility for bulk materials, Bulgaria

Despite their widespread practical use, cantilever steel systems are not explicitly defined in Eurocode 8, and specific seismic design provisions are not provided. Designers are therefore compelled to classify such systems within existing structural typologies, which may lead to inconsistencies in the selection of the behaviour factor q and in the adopted detailing strategy. The 2023 Kahramanmaraş earthquake sequence provides a unique opportunity to examine the real performance of such systems under extreme ground motion.

Recent studies following the 2023 Kahramanmaraş earthquakes have predominantly focused on reinforced concrete buildings (Yuzbasi, 2024; Ivanov & Chow, 2023; Isik et al., 2024), on material degradation (Bozdogan et al., 2024; Akca et al., 2024), on regional damage assessment (Altunsu et al., 2024), and on multi-storey steel frames (Tapia-Hernández et al., 2025). Although these contributions significantly advance the understanding of structural performance under extreme seismic demand, they do not provide a detailed analytical investigation of single-storey steel cantilever systems, nor do they propose calibrated seismic design parameters for such configurations.



a) Industrial building – distillery for processing of oil-essential raw materials, Medovo village. Source: TRIADA-BG (n.d.-a)



b) Public infrastructure – rehabilitation and modernization of the Kapitan Andreevo border checkpoint sheds. Source: TRIADA-BG (n.d.-b)

Fig. 2
Examples of cantilever structural systems in single-storey steel buildings for industrial and public applications

Georgiev (2024) reports on different types of damage observed in steel structures, including cantilever systems, and documents their generally good seismic performance; however, the study is limited to field observations without accompanying numerical analyses. The present study addresses this gap by integrating field observations with nonlinear dynamic analyses to clarify the governing response mechanism and propose rational design parameters within the Eurocode 8 framework. A structurally different type of cantilever system was examined by Thanopoulos et al. (2024), who investigated precast reinforced concrete industrial buildings affected by the same earthquake sequence. In those systems, the cantilever action is provided by RC columns with corbels supporting simply supported roof girders. The beam–column interface was identified as the critical vulnerability, exhibiting in-plane sliding, surface degradation at the contact zone, and a consequent loss of load-transfer capacity. In contrast to steel cantilever frames, which rely on controlled plastic hinge formation at the column base, the precast RC configuration displayed brittle behaviour governed primarily by deficiencies in joint detailing. These observations demonstrate that cantilever systems of different structural nature may develop fundamentally distinct seismic response mechanisms, with the precast RC typology being particularly sensitive at the beam–column connection.

The present study combines field observations from Antakya, analytical modelling, and nonlinear dynamic analyses based on recorded accelerograms to clarify the seismic response mechanism of single-storey steel cantilever structures. Based on this evidence, calibrated design parameters are proposed within the framework of Eurocode 8 to ensure controlled inelastic behaviour and reliable seismic performance.

Cantilever Systems in Seismic Design Standards

The provisions of EN 1998-1, Chapter 6 (CEN, 2004), are compared with the American standards AISC 341-16 (AISC, 2016) and ASCE 7-22 (ASCE, 2022).

American standards. AISC 341-16 explicitly defines two cantilever column systems: the Ordinary Cantilever Column System (OCCS) and the Special Cantilever Column System (SCCS). These systems differ primarily in ductility level and detailing requirements. A cantilever column system is defined as a seismic force-resisting system in which lateral forces are resisted by one or more columns cantilevered from the foundation. Such systems are conceptually similar to MRFs but are characterized by limited redundancy and concentration of plastic hinges at column bases. Their overstrength is minimal and primarily material-based, requiring conservative design assumptions. Since columns act as the dissipative elements, axial force demand is limited to 15% of the compressive resistance under design seismic conditions. For OCCS, no specific cross-section class limitations (compactness limitations) or protected zones are required, while weld detailing at the base is emphasized. SCCS

provisions are more restrictive: columns must be braced to ensure stable plastic hinging without lateral–torsional buckling, cross-sections must satisfy high ductility requirements, and protected zones are defined at the base. Critical welds are explicitly identified. The corresponding response modification parameters and height limitations are summarized in Table 1.

Table 1
Basic parameters for seismic design according to AISC (2016) and ASCE (2022)

Type of Cantilever system	Response Modification Coefficient, R	Overstrength Factor, Ω_0	Deflection Amplification Factor, C_d	Limitations of Structural Height, (m)
OCCS	1,25	1,25	1,25	10,66 In some cases, 20
SCCS	2,5	2,5	2,5	10,66

The explicit classification adopted in the American standards provides clear typological definition and calibrated seismic design parameters.

Eurocode 8. In contrast, EN 1998-1 (CEN, 2004), including its forthcoming second generation (EC8-2G), (CEN/TC 250, 2020), does not recognize cantilever column systems as a distinct structural typology. For single-storey buildings where lateral resistance is provided solely by cantilevered columns, the designer must select an interpretative design approach. Three alternatives may be considered:

a) Low Dissipative Structural Behaviour (LDSB). The system is designed essentially according to Eurocode 3, with limited reduction of seismic forces.

b) Classification as a Moment Resisting Frame (MRF). Plastic zones are assumed at column bases, provided the design axial force N_{Ed} in each column satisfies the inequality

$$N_{Ed} / N_{pl,Rd} < 0.3 \quad (1)$$

where $N_{pl,Rd}$ is the design plastic resistance to normal forces of the gross cross-section in accordance with EN 1993-1-1 (CEN, 2005). DCM or DCH may be selected, implying cross-section classes 1 and 2 (DCM) or class 1 (DCH). Capacity design is required for column base connections. However, due to the lack of redundancy, selection of the behaviour factor q requires engineering judgement, as the standard provides no explicit guidance.

c) Classification as an Inverted Pendulum (IP) system. DCM or DCH may again be adopted, influencing the behaviour factor q and the required cross-section class. Capacity design of the column base connection is required. For statically determinate cantilever systems, selecting DCH and considering the overstrength factor $\alpha_u \div \alpha_y = 1,1$ may lead to overestimation of the actual overstrength, since plastic hinging is generally confined to the column bases. It should be noted that EN 1998-1 (CEN, 2004) explicitly excludes certain one-storey frame configurations with interconnected column tops and limited axial force ratio (equation 1) from the IP category. This remark may lead inexperienced designers to disregard the IP interpretation entirely when assessing cantilever steel systems. Nevertheless, the standard does not provide specific guidance for such systems. The basic parameters associated with these approaches are summarized in Table 2.

Unlike the American standards, EN 1998-1 does not provide explicit classification or calibrated response factors for steel cantilever column systems. This leads to interpretative design choices, particularly regarding the behaviour factor q, expected ductility level, and overstrength assumptions. The comparative review demonstrates that while American provisions offer clear typological definition and consistent seismic parameters, Eurocode 8 leaves the design of steel cantilever column systems open to interpretation. This regulatory ambiguity motivates the need for analytical verification of their seismic response, addressed in the following sections through nonlinear dynamic analyses based on recorded ground motions.

Type of structural system	Behaviour factor, q	$\frac{\alpha_u}{\alpha_y}$	Deflection behaviour factor, q_d	Limitations
LDSB	1,5	*NA*	1,5	Eurocode 3 only
MRF - DCM	4,0	1,0	4,0	Equation (1)
MRF - DCH	5,0	1,1[a]	5,0	Equation (1)
IP - DCM	2,0	1,0	2,0	Equation (1)
IP - DCH	2,0	1,1[a]	2,0	Equation (1)

[a] - This option is not appropriate, as plastic hinges in steel cantilever systems are generally expected to form at column bases, resulting in inherently limited overstrength. *NA* – not applicable

Table 2

Basic parameters for seismic design according to EN 1998-1 (CEN, 2004)

Field Observations and Recorded Seismic Demand in Antakya

Following the 6 February 2023 earthquake sequence, an engineering reconnaissance mission of the National Earthquake Engineering Center (NEEC), in which the author participated (Georgiev, 2024), was conducted at the end of May 2023. The mission included inspections in several affected cities. The present study focuses on observations made in the new part of Antakya, within a residential area bounded by Atatürk and M. Kemal boulevards and the adjacent streets (**Fig. 3**). The inspected area is characterized predominantly by recently constructed reinforced concrete residential buildings, presumably constructed after 2002, many of which suffered severe damage or partial collapse. Within this context, two steel buildings with cantilever structural systems were identified and inspected: a car showroom complex and a single-storey grocery store (Georgiev, 2024). The latter is examined in detail, as its structural configuration corresponds directly to the cantilever system discussed in this study. The site is located between seismic stations 3123 and 3124, at distances of approximately 2 km and 1.2 km, respectively. The active fault lies approximately 2 km to the east–south of the site. Of particular relevance are the accelerograms recorded at station 3124 during the first earthquake of the sequence (Mw = 7.7, 04:17 local time). Basic data for the surrounding seismic stations are summarized in **Table 3**, while the horizontal acceleration time histories (EW and NS components) from station 3124 are shown in **Fig. 4**.

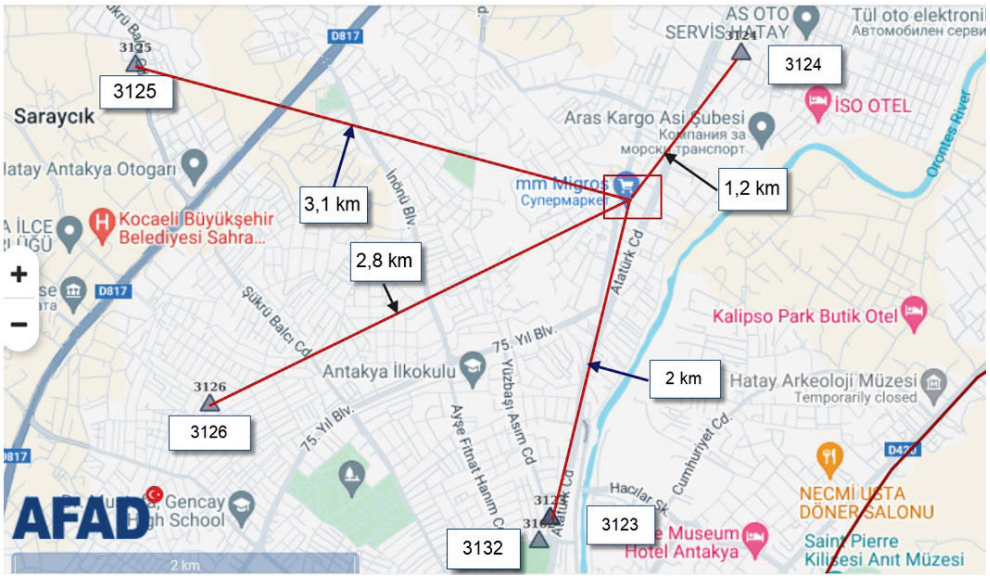


Fig. 3

Location of the case study site in Antakya and the nearest seismic stations (AFAD-TADAS, 2024)

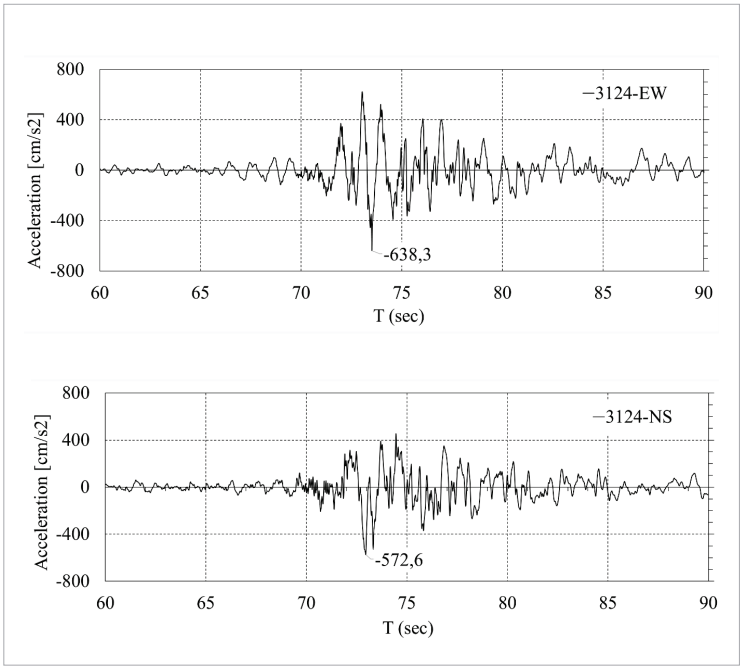
Table 3
Seismic stations basic data

Station №	Altitude (m)	Epicentral Distance (km)	V_{S30} (m/s)	Soil type (CEN, 2004)	Local site class (TSC-2007)
3123	85,0	143,00	469	B	Z2
3124	84,0	140,11	283	C	Z3
3125	156,0	142,15	448	B	Z2
3126	123,0	143,54	350	C	Z3
3132	104,0	143,12	377	B	Z2

To assess the difference between the recorded ground motion and the design seismic action prescribed by the Turkish Seismic Code, reference is made to TSC-2007. This choice is justified by the apparent construction period of the buildings in the investigated neighbourhood, which were most likely designed according to TSC-2007 rather than the more recent TSC-2018 provisions (AFAD, 2018). The acceleration time histories presented in **Fig. 4** indicate a pronounced strong-motion phase of approximately 25-30 seconds, with peak ground acceleration (PGA) occurring around 72–73 seconds from the start of the record. For the return period of 475 years and a soil factor S=1,15 corresponding to the ground conditions at station 3124, the design PGA according to TSC-2007 is approximately 1,15 × 0,4 × 981 = 451 cm/s^2. The recorded peak values are 638 cm/s^2 (EW component) and 572,5 cm/s^2 (NS component), exceeding the design PGA by 42% and 27%, respectively. Based on these values, the actual seismic demand at the site was greater than the 475-year design earthquake but remained below the Maximum Considered Earthquake corresponding to a 2475-year return period.

A more comprehensive assessment of seismic demand and the expected structural damage is obtained through analysis of the Elastic Response Spectra (ERS). The recorded spectra were compared with the code-prescribed ERS for return periods of 475 and 2475 years according to TSC-2007. Since TSC-2007 does not explicitly provide the ERS for a 2475-year return period, it was derived in this study by scaling the reference 475-year spectrum while preserving its shape (constant corner periods). The scaling factor γ was calculated using **equation (2)**.

Fig. 4
Acceleration time histories recorded at seismic station 3124: East–West (EW) and North–South (NS) components



$$\gamma \approx \left(\frac{T_{LR}}{T_L}\right)^{-\frac{1}{3}} \quad (2)$$

where: T_{LR} = 475 years corresponds to the reference seismic action with a 10% probability of exceedance in 50 years. T_L = 2475 years corresponds to the "Near Collapse" performance level. In the present analysis, γ = 1.73 was used. The spectral accelerations derived from the recordings at stations 3123 and 3124,

together with the code-based ERS, are presented in Figs. 5 and 6. For most of the relevant period range (T ≥ 0,4 s), the recorded spectral accelerations significantly exceed the design spectrum corresponding to the 475-year return period.

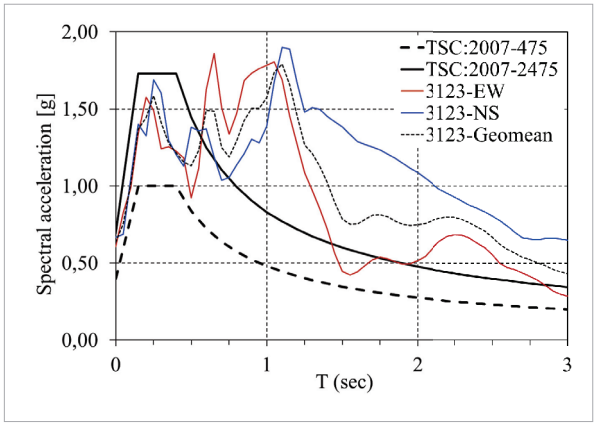


Fig. 5
Spectral accelerations from station 3123 compared with TSC-2007 elastic response spectra (AFAD-TADAS, 2024; Seismosoft, 2024)

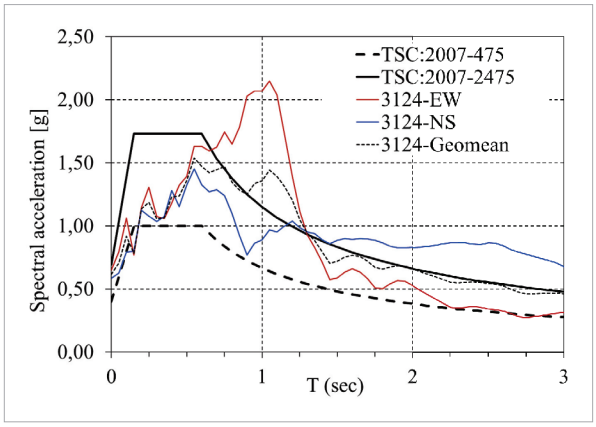


Fig. 6
Spectral accelerations from station 3124 compared with TSC-2007 elastic response spectra (AFAD-TADAS, 2024; Seismosoft, 2024)

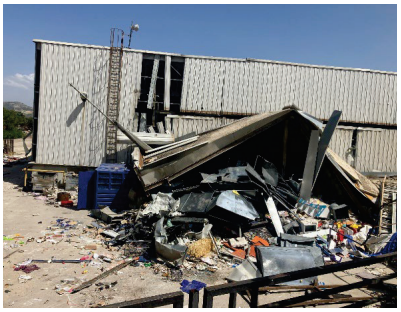
For a wide range of structural periods, particularly between 0,4 s and 1,5 s, the recorded spectral accelerations significantly exceed the code-prescribed values for the 475-year return period. This range is directly relevant to single-storey cantilever steel structures with fundamental periods typically between 0,8 s and 1,25 s. Under such demand levels, even well-designed structures would be expected to experience severe nonlinear response and potentially approach the Near Collapse limit state. Within this seismic context, the performance of the inspected single-storey grocery store building is of particular interest. Photographs before and after the earthquake are presented in Figs. 7 and 8. At the time of the author's inspection, debris from suspended ceilings and lightweight interior wall cladding was being removed, which allowed direct and unobstructed inspection of the structural system. No visible structural damage was observed in the primary steel frame. Significant damage was evident in the suspended ceilings and store equipment (Fig. 8c). The lateral force-resisting system consists exclusively of steel cantilever columns (Fig. 8b), spaced at 12 m in the longitudinal direction and 20 m in the transverse direction (Fig. 9b). The columns are fixed at their bases in both principal directions and enclosed for fire protection and architectural purposes. Structurally, they are battened built-up members composed of two channel sections connected by transverse plates. The interior retail and storage spaces (Fig. 8a, c) are structurally independent from the external steel frame, representing a building-within-a-building configuration. The roof system comprises lightweight primary and secondary trusses with unbraced bottom chords. Based on the low weight of the steel members and the modest regional snow loads, it is reasonable to assume that the roofing assembly consists of corrugated steel sheets, thermal insulation, and membrane waterproofing, resulting in minimal permanent load. While non-structural elements suffered severe damage and local collapse, no signs of local buckling or connection failure were detected in the primary structure. The canopy over the external loading ramp collapsed (Fig. 7b), likely due to instability of its supporting columns associated with a relatively heavier roof configuration (Georgiev, 2024). The absence of structural damage under seismic demand exceeding the design level provides the empirical basis for the subsequent analytical investigation of the seismic response mechanism of this steel cantilever system.

Fig. 7

Local grocery store building in Antakya, Atatürk Boulevard (Google, 2024; personal archive)



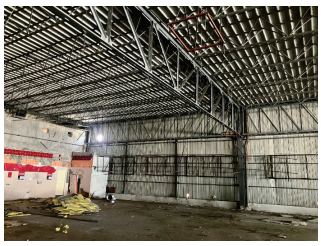
a) General view of Atatürk Boulevard in 2020, prior to the earthquake (Google, 2024)



b) View of the rear loading ramp in 2023, after the earthquake, showing the collapse of the canopy

Fig. 8

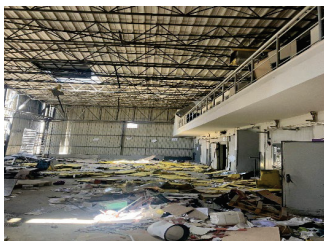
Interior damage and partial demolition of the local grocery store building, Antakya, Atatürk Boulevard (personal archive)



a) Interior view of the retail area



b) Cantilever column and roof truss system



c) Interior view of the storage area

Analytical Investigation of the Seismic Response Mechanism

The observations in Antakya raise a fundamental engineering question. The recorded ground motion exceeded the design seismic parameters prescribed by the code. Such exceedance should not be regarded as unexpected, but rather as a reminder that earthquake demand may surpass anticipated levels (Paulay & Priestley, 1992). At the same time, the inspected steel structure was not explicitly designed for high ductility or significant overstrength. Nevertheless, it survived the strong earthquake without structural collapse. To reconcile these observations, a series of analytical investigations was undertaken.

Modal analysis. The first step of the analytical investigation consisted of developing a numerical model of the external structural system for elastic modal analysis. The internal mezzanine structure was excluded from the model, as it is structurally independent from the primary frame. Based on site photographs and dimensional estimation using Google Maps, the building plan was reconstructed with axial spacing of 2 @ 20 = 40 m in the transverse direction and 5 @ 12 = 60 m in the longitudinal direction. The clear height from finished floor level to the underside of the roof trusses was assumed to be 4.50 m (**Fig. 9**). Member cross-sections were inferred from photographic evidence and verification of vertical load-carrying capacity. Based on the observed structural configuration, typical construction practice for similar buildings, and engineering judgement, steel properties corresponding to grade S275 for the UPE sections and S235 for the angle sections were assumed. The resulting member sections for the columns and truss elements are presented in **Table 4** and **Fig. 10.** All columns were modelled as fixed at their bases about both principal axes, while the column-to-truss connections were assumed pinned. Gravity loads, enclosure loads, and corresponding seismic masses are summarized in **Table 5**. A three-dimensional model of the external frame was developed, and modal analysis was performed. The fundamental periods

were obtained as $T_{1,X}$ = 0,95 s (longitudinal direction) and $T_{1,Y}$ = 1,08 s (transverse direction). Even considering modelling uncertainty, these periods fall within the range where the recorded spectral accelerations from station 3124 (**Fig. 11**) are particularly high. Comparison with TSC-2007 (AFAD, 2007) indicates that the seismic demand is close to the Maximum Considered Earthquake (DD1, 1/2475) and clearly exceeds the design earthquake level DD2 (1/475). Within the period range 0,80–1,25 s, the NS component produces spectral accelerations between DD2 and DD1, while the EW component consistently exceeds the DD1 spectrum. This amplification is attributed to pulse-like ground motions, basin effects, and supershear rupture phenomena reported for the Antakya region Gani et al. (2025). From an engineering perspective, the implication is clear: the structure was subjected to seismic demand approaching or exceeding the maximum code-based design level. Survival under such demand is likely to require activation of reliable energy dissipation mechanisms without loss of global stability.



a) Plan dimensions identified from satellite imagery (Google, 2024)



b) Identification of principal framing dimensions

Fig. 9

Local grocery store building: plan and main structural dimensions

Member	Cross-section	Characteristic spacing parameter (mm)	Material yield strength (MPa)	Comment
Internal Column	2UPE 240	200*	275	battened
External Column	2UPE 240	-	275	battened, rotated 90°
Truss top chord	2L 70x5	10*	235	-
Truss bottom chord	2L 60x6	10*	235	-
Truss diagonals and verticals	2L 40x4	10*	235	-

Table 4

Cross-sections and material properties of structural members

* For built-up columns, the value represents the centre-to-centre distance between component sections.

* For double-angle members, it represents the clear distance between the inner faces of the angles.

Building sub-part	Load (kN/m²)	Tributary area (m²)	Seismic mass (t)	Total seismic mass per frame (t)
Roof cladding and insulation	0.35	480	17.125	28.500
Roof structural steel	0.06	480	2.936	
Suspended ceiling	0.10	480	4.893	
Steel columns	0.05	480	2.446	
Façade cladding	0.10	108	1.101	

Table 5

Gravity loads and corresponding seismic masses per transverse frame

Fig. 10

Transverse frame configuration and built-up column cross-sections

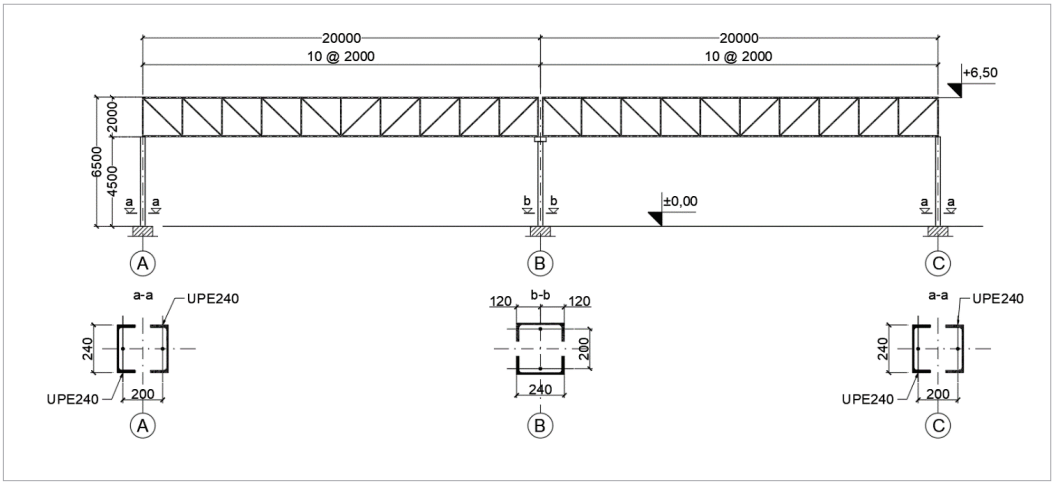
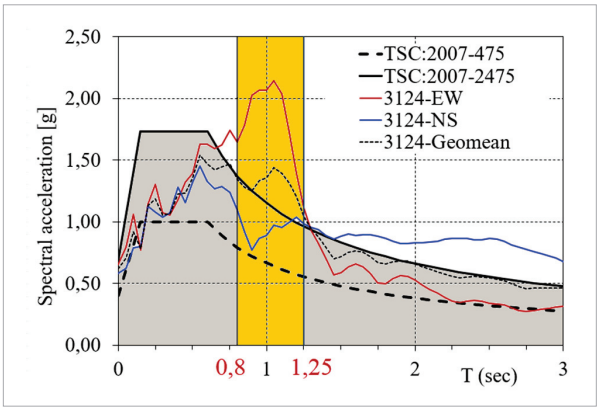


Fig. 11

Comparison of elastic response spectra derived from station 3124 recordings with the TSC-2007 spectrum for periods between 0,8 s and 1,25 s



Dynamic Linear Analysis. As indicated by the mass evaluation in **Table 5**, the structure is relatively lightweight. For comparison, similar buildings in Bulgaria, subjected to higher snow loads and stricter thermal insulation requirements, would typically have nearly twice the dead load. Owing to this low mass, the possibility that the structure responded predominantly in the elastic range during the Kahramanmaraş–Pazarcık earthquake was examined. A dynamic linear analysis (DLA) was therefore performed using the EW component of the accelerogram recorded at station 3124 as input motion. Rayleigh damping was adopted with a modal damping ratio of 5% assigned to the first and second vibration modes. The numerical model was developed in SAP2000 (CSI, 2010). Representative results of the DLA are presented in **Fig. 12**. Total seismic mass per transverse frame is M = 28,5 t. Maximum Base Shear (BS) force reached 400,5 kN at second 75. The fundamental period of the 2D model is T_1=1,17 s. The maximum spectral acceleration corresponding to the elastic structural response $S_{e,max}$ was determined using **formula (3)**.

$$Se,\max = \frac{BS}{M} = \frac{400,5}{28,5} = 14,05\frac{m}{s^2} = 1,43g \quad (3)$$

A comparable estimate can be obtained directly from **Fig. 11** by reading the spectral ordinate corresponding to a period of 1,17 s. The bending moments at the base of the internal column, assuming elastic response with 5% damping, reach 620 kN·m and –608 kN·m, respectively (**Fig. 12b**). Such demand levels exceed the available flexural resistance of the column under the combined axial force and bending interaction. The resulting strength deficit is substantial, making a purely elastic structural response unrealistic. Consequently, an alternative response mechanism involving inelastic behaviour must be considered to explain the observed structural survival under this strong ground motion.

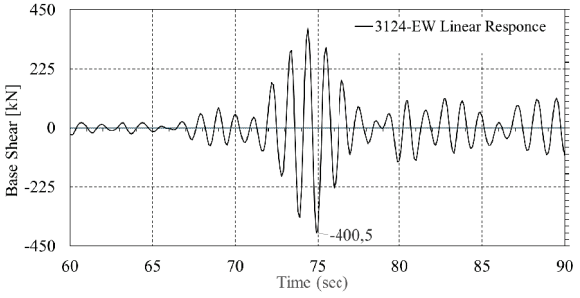
Dynamic Non-linear Analysis. To investigate the structural response beyond the elastic range, a nonlinear model was developed. A concentrated plasticity approach was adopted, with plastic hinges assigned at the base of each column. The backbone curve was defined using an expected material

yield strength of 295 MPa, together with the corresponding plastic moment capacity of the cross-section. Bilinear isotropic hardening was adopted, with the slope of the post-yield branch taken as approximately 0,04 of the initial elastic stiffness in order to account for strain hardening effects. Although the columns are built-up battened members, their overall configuration resembles a box-type section. Lateral–torsional buckling was therefore assumed to be restrained. This assumption is supported by field observations, which did not indicate instability or out-of-plane deformation of the columns after the earthquake. The results of the dynamic nonlinear analysis (DNA) and their comparison with the dynamic linear analysis (DLA) are presented in **Fig. 13**.

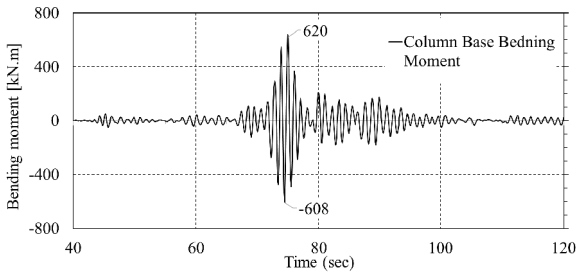
The total seismic mass and fundamental period of the 2D model remain unchanged from the previous analysis. The maximum base shear obtained from the DNA is 144,0 kN. The corresponding maximum acceleration of the seismic mass $S_{e,max}$ for the nonlinear response was determined using **equation (4)**.

$$Se,\max = \frac{BS}{M} = \frac{144}{28,5} = 5,05\frac{m}{s^2} = 0,515g \quad (4)$$

The resulting maximum acceleration of the seismic mass is 2,776 times lower than that obtained from the elastic analysis (**Eq. 3**). This significant reduction is attributed to energy dissipation through the development of plastic strains at the column bases. The analysis confirms that the structure responded inelastically and developed considerable residual displacements (**Fig. 13b**). Considering the building layout (**Fig. 9a**), the transverse frame is more closely aligned with the NS ground motion component. Therefore, subsequent analyses are performed using the NS record and explicitly accounting for second-order (P–Δ) effects.



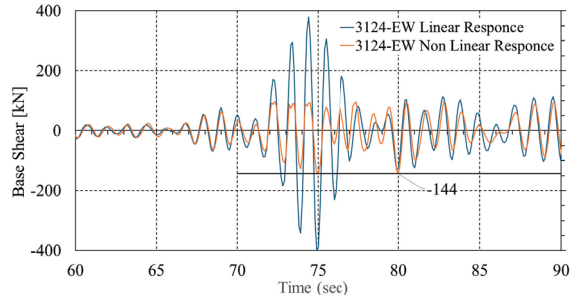
a) Base shear time history



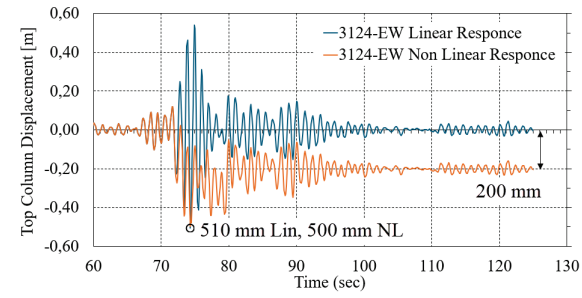
b) Time history of the bending moment at the base of the internal column

Fig. 12

Base shear and column base bending moment time histories from DLA using the 3124-EW record



a) Base shear time history



b) Top column displacement time history

Fig. 13

Comparison of top column displacements and base shear time histories under the 3124-EW accelerogram obtained from DLA and DNA

Fig. 14

Total base shear time history under the 3124-NS accelerogram (second-order DNA)

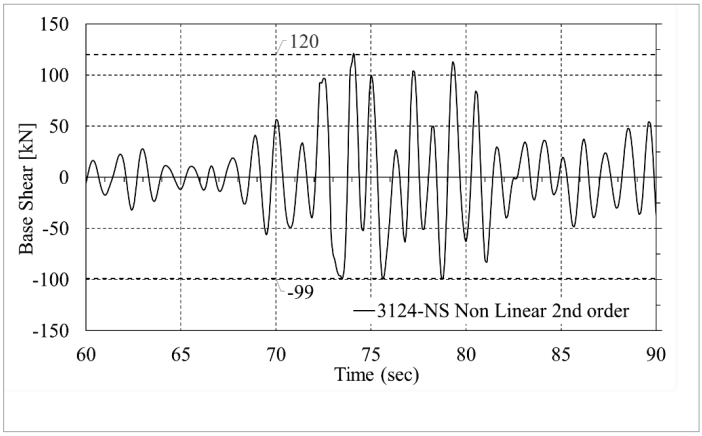
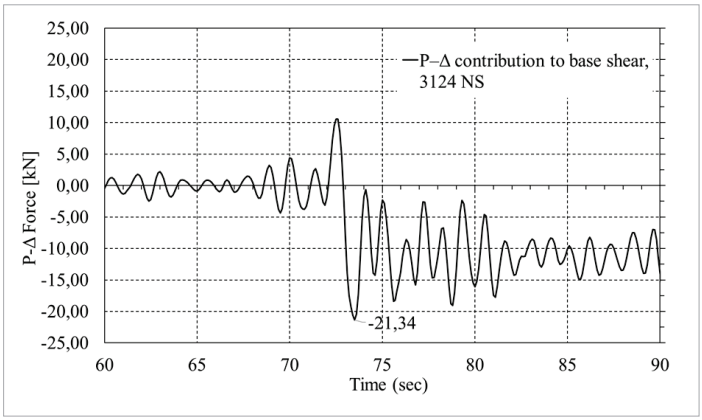


Fig. 15

P–Δ contribution to base shear under the 3124-NS accelerogram (second-order DNA)



Dynamic Nonlinear Analysis with P–Δ Effects.

The same numerical model was employed to account for second-order effects. A leaning column approach was adopted, whereby the entire vertical load associated with the studied frame under the seismic design situation was applied to capture global P–Δ effects. The seismic excitation was introduced using the NS component of the 3124 accelerogram. The resulting time histories of total base shear (TBS) and the P–Δ contribution obtained from the second-order dynamic nonlinear analysis are presented in **Figs. 14** and **15**.

The results indicate that, for a maximum total base shear of 120 kN, approximately 20 kN is attributable to second-order effects. These values enable estimation of the interstorey drift sensitivity coefficient θ in accordance with Eurocode 8 (CEN, 2004), calculated using equations (5) and (6).

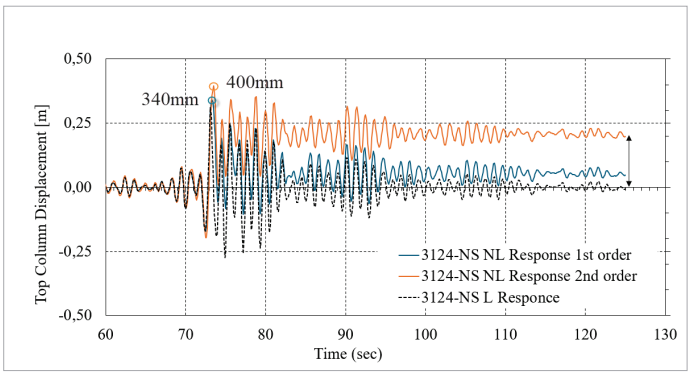
$$TBS = K_\theta \times BS^{1st\ order} \rightarrow 120 = K_\theta \times 100 \rightarrow K_\theta = 1,20 \quad (5)$$

$$K_\theta = \frac{1}{1-\theta} \rightarrow 1,2 = \frac{1}{1-\theta} \rightarrow \theta = 0,167 \quad (6)$$

A comparison of all dynamic analyses is presented in **Fig. 16**. The structure exhibits clear sensitivity to second-order effects. When the coefficient θ is determined based on displacements, a value of 0,15 is obtained from equation (7). When evaluated from the ratio of second-order base shear contribution to total base shear, θ=0,167, equation (6). These results confirm that neglecting second-order effects would lead to underestimation of horizontal displacements. Since the lateral force-resisting elements have developed plastic strains, the structure exhibits limited re-centering capability and experiences significant residual drifts. Omission of

Fig. 16

Top column horizontal displacement time histories under the 3124-NS accelerogram for different dynamic analysis approaches



P–Δ effects would therefore substantially underestimate the residual top-column displacements. The governing response mechanism is therefore characterized by controlled plastic hinging at column bases combined with significant P–Δ amplification and limited re-centering capacity.

$$K_\theta = \frac{400}{340} = \frac{1}{1-\theta} \rightarrow \theta = 0{,}15 \quad (7)$$

Proposed Eurocode 8 Design Approach for Cantilever Systems: Case Study and Validation

The analyses presented in the previous section indicate that the survival of the structure can be attributed to the development of ductile plastic hinges at the column bases, without triggering lateral–torsional buckling or global instability. This observation raises the question of how steel cantilever systems should be designed. Unlike ANSI/AISC 341-16 and ASCE/SEI 7-22, Eurocode 8 (CEN, 2004) does not define steel cantilever systems as a distinct structural typology and does not provide explicit design provisions for such configurations. As discussed in Section 2, none of the interpretative options currently available under EN 1998-1 fully resolves the associated design ambiguities. The present study therefore proposes that steel cantilever systems be treated as a specific subtype of moment-resisting frames (MRFs) within the Eurocode 8 framework. When applying response spectrum analysis (RSA) according to EN 1998-1, the key design parameters summarized in **Table 6** are recommended. A comparable conceptual approach is adopted in the United States, where AISC 341-16 (AISC, 2016) explicitly distinguishes between Ordinary and Special Cantilever Column Systems (OCCS and SCCS), calibrated according to their global ductility capacity (see **Table 1**). The proposed parameters reflect the limited redundancy and concentrated plasticity of steel cantilever systems, while ensuring a controlled and stable inelastic response at the column bases.

Table 6

Proposed seismic design parameters for Steel Cantilever Systems (SCS) under EN 1998-1 (CEN, 2004)

SCS, ductility class	Behaviour factor, q	Overstrength factor, $\Omega_0 = \frac{\alpha_u}{\alpha_y}$	Deflection behaviour factor, q_d	Column cross-section class	Additional design requirements
SCS - DCM	2,0	1,0	2,5	Class 1 and 2	Requirements (b) and (c)

[b] The axial force ratio $N_{Ed}/N_{pl,Rd}$ shall be limited to avoid significant reduction of the plastic bending resistance

[c] Lateral–torsional and global buckling of columns shall be prevented through appropriate cross-sectional configuration or adequate bracing

To evaluate the proposed design approach, a case study (CS-1) was developed. The transverse frame geometry shown in **Fig. 10** and the gravity loads summarized in **Table 5** were adopted. The structure was designed in accordance with Eurocode 8 (CEN, 2004), assuming ductility class DCM, importance factor $\gamma_I = 1{,}0$, ground type *C* with soil factor *S* = 1,15, design ground acceleration on type A ground $a_{g,r} = 0{,}4 \times 9{,}81 = 3{,}924$ m/s^2 and behaviour factor *q*=2,0.

The columns were selected as hollow structural sections SHS 300×10 in accordance with EN 10210 (CEN, 2019), satisfying the width-to-thickness requirements for cross-section class 1. Modal analysis and single-component response spectrum analysis (RSA) were performed to determine the seismic effects. The main parameters adopted for the seismic analysis are summarized in **Table 7**, while the resulting design actions and resistance checks are presented in **Table 8**. Although the analytical model is two-dimensional, it should be emphasized that the columns constitute the only lateral force-resisting elements. In reality, they are subjected to axial force and biaxial bending resulting from the two horizontal components of seismic action. This effect is considered in the design by verifying the axial–flexural interaction resistance. The design bending moments about the two principal axes were combined using the 100–30% rule according to EN 1998-1.

Table 7

Seismic response parameters of the cantilever system (Case Study CS-1)

Case study ID	Seismic Mass (t)	Fundamental period T_1 (s)	Base Shear (kN)	Max. storey displacement (Δ_{el}, m)	Interstorey drift ratio (-)	Column cross-section class	Axial force ratio $N_{Ed}/N_{pl,Rd}$
CS-1	26,74	0,554	146,65	0,044	0,0068 ≤ 0,0075	Class 1	0,048 < 0,30

Table 8

Column design verification results after response spectrum analysis (RSA)

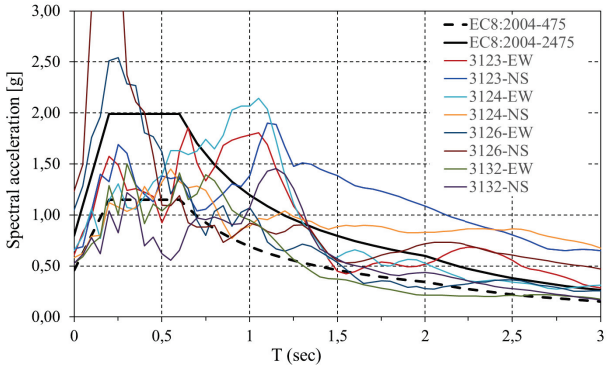
Column	Section	Material	Utilization ratio	Governing check	Second-order sensitivity coefficient (θ)
External	SHS 300x10	S235H	0,907	Bending	0,0363 < 0,10
Internal	SHS 300x10	S235H	0,793	Bending	0,0363 < 0,10

The design results confirm compliance with DCM requirements and limited sensitivity to second-order effects under RSA.

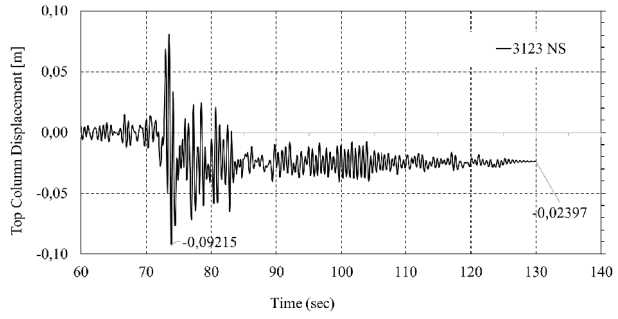
Following the RSA-based design according to the proposed approach, a series of eight dynamic nonlinear analyses (DNAs) was carried out. The analyses accounted for both material and geometric nonlinearity and were performed using real accelerograms recorded during the Kahramanmaraş–Pazarcık earthquake. Only records from stations located within the city of Antakya–namely 3123, 3124, 3126, and 3132–were considered, using both the EW and NS components. No amplitude scaling or spectrum matching was applied; the accelerograms were used in their original recorded form as provided by AFAD-TADAS (2024). **Fig. 17** presents the Eurocode 8 elastic response spectrum for soil type C, together with the spectra derived from the selected recordings, as well as a representative top-column displacement time history obtained from DNA using the 3124-NS record. To capture the full decay of structural oscillations and accurately quantify residual storey displacements, each accelerogram was extended by 5 s with zero acceleration. The principal response parameters obtained from the nonlinear analyses are summarized in **Table 9**.

Fig. 17

CS-1: elastic response spectra and representative nonlinear displacement response



a) Eurocode 8 elastic response spectrum (soil type C) and spectra derived from recordings 3123, 3124, 3126, and 3132



b) Top column displacement time history under the 3124-NS accelerogram, showing maximum interstorey drift (MID) and residual displacement

The column base rotation was evaluated using the chord rotation method, defined as the ratio of the maximum storey displacement to the column height. This approach provides a conservative estimate of the plastic rotation demand, as the elastic component of the displacement is not subtracted. The interstorey drift sensitivity coefficient θ was calculated considering the maximum axial force in the horizontal element connecting the structural frame to the leaning

column (see Table 9, last column). In these analyses, the nominal yield strength of S235 steel, fy = 235 MPa, was adopted.

Table 9
Nonlinear seismic response parameters of CS-1 under recorded ground motions, f_y=235 MPa

ID	Recording	Maximum storey displacement (m)	Residual storey displacement (m)	Residual drift ratio (%)	Maximum base shear (kN)	Column base rotation (mrad)	Second-order sensitivity coefficient θ
1	3123 EW	0,083	0,0234	0,52	198,3	18,4	0,0301
2	3123 NS	0,131	0,0365	0,81	211,2	29,1	0,0374
3	3124 EW	0,117	0,0113	0,25	215,5	26,0	0,0325
4	3124 NS	0,084	0,0119	0,26	194,8	18,7	0,0257
5	3126 EW	0,118	0,0560	1,24	210,7	26,2	0,0336
6	3126 NS	0,108	0,0452	1,01	202,8	24,0	0,0322
7	3132 EW	0,080	0,0128	0,29	201,4	17,8	0,0240
8	3132 NS	0,042	0,0004	0,09	137,1	9,33	0,0182

The results indicate stable inelastic behaviour with column base rotations up to 29 mrad, moderate residual drifts, and limited second-order sensitivity (θ < 0,04), confirming adequate global stability. The observed nonlinear performance supports the proposed behaviour factor q = 2.0 and demonstrates that steel cantilever systems designed according to the suggested framework can achieve controlled inelastic response without loss of global stability.

Discussion and Validation of the Proposed Eurocode 8 Design Parameters

The eight dynamic nonlinear analyses (DNAs) indicate that plastic hinges developed at the bases of all three columns for seven of the records. Only the 3132-NS record resulted in a purely elastic response (Table 9, last row). Since no inelastic behaviour was triggered in this case, it is excluded from the statistical evaluation presented in this section. Table 10 summarizes the arithmetic mean and maximum values of the key response parameters obtained from the seven inelastic analyses.

Table 10
Mean and maximum values of key nonlinear seismic response parameters

	Maximum storey displacement (m), MID	Residual storey displacement (m)	Residual drift ratio (%)	Maximum Base Shear (kN)	Column base rotation (mrad)	Second-order sensitivity coefficient θ
Mean value	0,103	0,028	0,63	205,0	22,9	0,0310
Max value	0,131	0,056	1,24	215,5	29,1	0,0374
Max/Mean ratio	1,27	2,0	1,97	1,05	1,27	1,21

The results presented in Tables 9 and 10 indicate that the largest dispersion is observed in the residual storey displacements. This parameter appears to be governed primarily by record-specific characteristics rather than by the magnitude of PGA or the spectral acceleration $Sa(T_1)$. Notably, the largest residual displacement is associated with record 3126-EW, whereas the maximum storey displacement occurs under record 3123-NS. The variability of maximum storey displacements and column base rotations, expressed through the Maximum-to-Mean ratio, remains within approximately 30%. These differences reflect the inherent variability of the input ground motions. In contrast, the variation in base shear is limited to about 5%, indicating a stable global response of the structural system. This limited dispersion can be attributed to the structural simplicity of the steel cantilever system and the consistent formation of plastic hinges at all column bases. The small differences in base shear are primarily related to variations in post-yield hardening due to

material strain hardening. The relationship between the parameters obtained from RSA-based design and those derived from the nonlinear dynamic analyses (DNA) is particularly important for validation of the proposed design framework. Table 11 presents the calculated displacement behaviour factor q_d and the total overstrength Ω, evaluated from the seven inelastic records using equation (8). The total overstrength Ω is decomposed into two components. The first component is the design overstrength Ω_d, which reflects the conservatism inherent in the design procedure. The second component is the inherent system overstrength Ω_0, arising from force redistribution during the development of a global plastic mechanism and from strain hardening of the material. The overstrength is evaluated using equation (9). The design overstrength Ω_d was determined by assuming simultaneous attainment of the plastic bending moment at the bases of all three columns. The corresponding shear force, required to produce this state for a column height of 4,5 m, is calculated and compared with the base shear obtained from RSA. The resulting ratio is 1,348, representing Ω_d , while the inherent system overstrength Ω_0 is subsequently derived from equation (9).

$$q_d = \frac{MID}{\Delta_{el}} \quad (8)$$

$$\Omega = \Omega_d \times \Omega_0 \quad (9)$$

Table 11

Displacement behaviour factor q_d and overstrength components derived from nonlinear dynamic analyses

Recording	Max. storey displacement (m), MID	q_d (-)	Max. base shear, DNA (kN)	Max. base shear, RSA (kN)	Total over-strength Ω (-)	Design overstrength Ω_d (-)	Inherent system over-strength Ω_0 (-)
3123 EW	0,083	1,886	198,3	146,7	1,352	1,348	1,003
3123 NS	0,131	2,977	211,2	146,7	1,440	1,348	1,068
3124 EW	0,117	2,659	215,5	146,7	1,469	1,348	1,090
3124 NS	0,084	1,909	194,8	146,7	1,328	1,348	0,985
3126 EW	0,118	2,682	210,7	146,7	1,436	1,348	1,065
3126 NS	0,108	2,455	202,8	146,7	1,382	1,348	1,026
3132 EW	0,080	1,818	201,4	146,7	1,373	1,348	1,018
Mean value	0,103	2,341	204,96	146,7	1,397	1,348	1,036

Table 12 compares the key parameters obtained from RSA-based design with the mean values derived from the seven nonlinear dynamic analyses. The proposed displacement behaviour factor q_d, provides a satisfactory estimate of the actual displacement demand, with the mean value from DNAs remaining close to the adopted design value. The interstorey drift sensitivity coefficient θ, calculated according to Eurocode 8 (CEN, 2004) and evaluated from the nonlinear analyses, also shows good agreement with the RSA-based estimate. With respect to overstrength, Eurocode 8 associates the behaviour factor q primarily with the inherent system overstrength Ω_0, rather than the design overstrength Ω_d. The mean value obtained from DNAs ($\Omega_0 \approx 1,04$) supports the suitability of the proposed value $\Omega_0=1,0$.

Overall, the analytical results and the stable inelastic response observed for the cantilever frame CS-1 support the proposed behaviour factor q=2,0 for ductility class DCM as a rational and sufficiently conservative design choice.

The RSA-based design parameters are either closely aligned with or slightly conservative relative to the mean nonlinear response, indicating a consistent and rational calibration of the proposed framework.

Table 12
Comparison of RSA design parameters with mean values from nonlinear dynamic analyses

Parameter	Mean value (7 DNAs)	RSA design value
Displacement behaviour factor q_d	2,341	2,500
Inherent system overstrength factor Ω_0 ($\frac{\alpha_u}{\alpha_y}$)	1,036	1,000
Second-order sensitivity coefficient θ	0,0310	0,0363

Conclusions

Steel cantilever systems can be applied in regions of high seismic hazard, provided that appropriate design constraints are satisfied. Field observations from the 2023 Kahramanmaraş–Pazarcık earthquake in Antakya confirm that such systems are capable of surviving severe ground motions. The investigations presented in this study explain the mechanisms that enabled the observed structural survival. Although certain modelling assumptions were necessary due to incomplete geometric and material data (Boshnakov, 2022), the results provide a consistent basis for understanding the seismic behaviour of this class of structures. The seismic performance of steel cantilever systems is governed by the controlled development of plastic hinges at the column bases. Two principal design strategies may be adopted. The first approach, adopted in this study, directs plastic deformations into the column section immediately above a strong and capacity-designed base joint, requiring adequate stiffness and connection detailing. An alternative approach, supported by Raykov (2014, 2015), allows plastic deformation to develop within the base region itself, emphasizing the ductility of anchor bolts and grout. Although this solution may offer practical advantages, it requires further validation and appropriate calibration of the behaviour factor q.

In all cases, the global plastic mechanism is characterized by base hinging, and column stability under large displacements must be ensured. Hollow sections (SHS or RHS) are generally more suitable due to their favourable stability characteristics, whereas the use of open sections (HEA, HEB, IPE) requires further investigation. Particular attention must be paid to axial force levels in the columns, as excessive compression may significantly reduce plastic flexural capacity.

Eurocode 8 (CEN, 2004) does not explicitly define cantilever structural systems or provide dedicated design provisions for them. In practice, designers may classify such systems as moment-resisting frames (MRFs), inverted pendulum (IP) systems, or adopt a low-ductility structural behaviour (LDSB) approach. The latter may be inappropriate for seismic applications, as it relies primarily on Eurocode 3 (CEN, 2005) without enforcing capacity design at the column base. This may result in underestimation of the base joint resistance and the development of brittle failure mechanisms. The present study proposes treating steel cantilever systems as a distinct subtype of MRFs, recognizing their limited ductility compared to conventional multi-storey frames. Based on the performed nonlinear dynamic analyses, design values of q = 2,0 and q_d = 2,5 are recommended for inclusion within the Eurocode 8 framework.

Cantilever systems exhibit significant deformability, and compliance with the Damage Limitation State (1/95) criteria of Eurocode 8 (CEN, 2004) is therefore essential. Based on the present study, the allowable interstorey drift should be limited to 0,0075 h, even when façade systems can accommodate larger displacements, since other non-structural components remain vulnerable (Kardjiev, 2016; Georgiev, 2024). Owing to the system's deformability, P–Δ effects should be explicitly considered in RSA-based design, even in cases where Eurocode 8 does not mandate their inclusion.

This study is grounded in field observations from Antakya following the 2023 Kahramanmaraş–Pazarcık earthquake and is based entirely on unscaled recorded accelerograms. The results demonstrate that steel cantilever systems can dissipate seismic energy through limited ductility and survive severe ground motions. Further research is required to extend these findings. Priorities include bidirectional nonlinear analyses with simultaneous seismic components, evaluation of higher ductility classes, application of broader suites of ground motions, and detailed investigation

of column base detailing capable of sustaining the required plastic rotations. Additional attention should be given to robust roof beam–column joints under large displacements and to the influence of axial force on second-order sensitivity and plastic flexural capacity.

The analytical and field evidence confirms that steel cantilever systems can be reliably applied in regions of high seismic hazard when properly detailed. However, these findings should not be indiscriminately extended to cantilever systems constructed from prefabricated reinforced concrete elements. Their performance during the Kahramanmaraş earthquake sequence was highly unsatisfactory (Thanopoulos et al., 2024; Georgiev, 2025) and warrants further investigation and improvement.

The presented investigation should be regarded as an initial analytical study focused on identifying the governing response mechanism and proposing design implications for steel cantilever systems within the Eurocode 8 framework. The performed nonlinear analyses, based on seven unscaled recorded accelerograms, provide encouraging evidence regarding the proposed design parameters. Nevertheless, broader validation would require additional structural configurations, larger sets of seismic records, fully bidirectional nonlinear analyses, and refined modelling of the column-base region.

Acknowledgments

This study benefited from a field mission to the affected regions of İskenderun, Antakya, Kahramanmaraş, and Pazarcık in southeastern Türkiye in May 2023, organized by the National Earthquake Engineering Center (NEEC) at the University of Architecture, Civil Engineering and Geodesy (UACEG). The mission was funded under the National Roadmap for Scientific Infrastructure 2020–2027 program, coordinated by the National Institute of Geophysics, Geodesy and Geography at the Bulgarian Academy of Sciences. The author gratefully acknowledges his colleagues from NEEC for their collaboration during the field investigation and the subsequent analytical work. Appreciation is also extended to the funding institution for its financial support.

Use of Artificial Intelligence Tools

During the preparation of this manuscript, the author used ChatGPT (OpenAI) for language editing and text clarity improvements. The author reviewed all content and assumes full responsibility for the manuscript.

References

AFAD-TADAS. (2024). Turkish Accelerometric Database and Analysis System. https://tadas.afad.gov.tr/map

Akca, A. H., Sahin, O., Koc, K., & Aygörmez, Y. (2024). Mechanical and microstructural investigations on concrete of the collapsed buildings after Kahramanmaraş earthquakes. Engineering Science and Technology, an International Journal, 56, 101784. https://doi.org/10.1016/j.jestch.2024.101784

Altunsu, E., Güneş, O., Öztürk, S., Sorosh, S., Sarı, A., & Beeson, S. T. (2024). Investigating the structural damage in Hatay province after Kahramanmaraş-Türkiye earthquake sequences. Engineering Failure Analysis, 157, 107857. https://doi.org/10.1016/j.engfailanal.2023.107857

American Institute of Steel Construction (AISC). (2016). Seismic provisions for structural steel buildings (ANSI/AISC 341-16). AISC.

American Society of Civil Engineers (ASCE). (2022). Minimum design loads and associated criteria for buildings and other structures (ASCE/SEI 7-22). ASCE.

Boshnakov, K. (2022). Otnosno vazmozhnostite za standartizirane na kontrola varhu tochnostta na rezultatite ot chislen analiz na stroitelni konstruktsii [On the perspectives of standardizing the control over the accuracy of results of numerical analysis of building structures]. Bulgarian Journal for Engineering Design, (45), 89-97. https://bjed.tu-sofia.bg/items/BJED-0045(2022).pdf

Bozdogan, O., Erdag, A., & Ozdemir, A. (2024). Determination of mechanical properties of concrete and steel materials taken from buildings in Antakya after the Kahramanmaraş earthquakes. Case Studies in Construction Materials, 21, e03445. https://doi.org/10.1016/j.cscm.2024.e03445

Computers and Structures, Inc. (2010). SAP2000 (Version 14.1) [Computer software]. CSI.

Disaster and Emergency Management Authority (AFAD). (2018). Turkish building seismic code (TSC 2018). Ministry of Interior.

European Committee for Standardization (CEN). (2004). EN 1998-1:2004 Eurocode 8: Design of structures for earthquake resistance - Part 1: General rules, seismic actions and rules for buildings.

European Committee for Standardization (CEN). (2005). EN 1993-1-1:2005 Eurocode 3: Design of steel structures - Part 1-1: General rules and rules for buildings.

European Committee for Standardization (CEN). (2019). EN 10210-1:2019 Hot finished structural hollow sections of non-alloy and fine grain steels - Part 1: Technical delivery conditions.

European Committee for Standardization (CEN/TC 250). (2020). prEN 1998-1-2:2020 Eurocode 8: Design of structures for earthquake resistance - Part 1-2: Rules for new buildings.

Gani, E., Öztürk, S., & Sarı, A. (2025). Examination of the severe impact of the February 6, 2023 earthquakes on Antakya district considering pulse-like ground motions, supershear rupture, and basin effects. Soil Dynamics and Earthquake Engineering, 198, 109608. https://doi.org/10.1016/j.soildyn.2025.109608

Georgiev, T. (2024). Field observations and assessment of performance level of steel structures after the Kahramanmaraş earthquake sequence of 2023. In Proceedings of the International Conference on the Behaviour of Steel Structures in Seismic Areas (pp. 633-645). Springer Nature. https://doi.org/10.1007/978-3-031-62888-7_55

Georgiev, T. (2025). Some lessons from the Kahramanmaraş earthquake sequence of 2023 relevant to the Bulgarian construction practice. In N. Dobrinkova & S. Fidanova (Eds.), Environmental Protection and Disaster Risks (EnviroRisks 2024) (Lecture Notes in Networks and Systems, Vol. 883). Springer. https://doi.org/10.1007/978-3-031-74707-6_38

Google. (2024). Google Maps [Map]. https://www.google.com/maps

Isik, E., Hadzima-Nyarko, M., Radu, D., & Bulajić, B. (2024). Study on effectiveness of regional risk prioritisation in reinforced concrete structures after earthquakes. Applied Sciences, 14, 6992. https://doi.org/10.3390/app14166992

Ivanov, M. L., & Chow, W. K. (2023). Structural damage observed in reinforced concrete buildings in Adiyaman during the 2023 Turkiye Kahramanmaras earthquakes. Structures, 58, 105578. https://doi.org/10.1016/j.istruc.2023.105578

Kardjiev, V. (2016). Izsledvane povedenieto na nekonstruktivni elementi pri seizmichni vazdeystviya [Study of the behaviour of non-structural elements under seismic actions]. University of Architecture, Civil Engineering and Geodesy Press.

Ministry of Public Works and Settlement. (2007). Turkish earthquake code (TEC-2007): Specifications for buildings to be built in seismic areas. Government of Türkiye.

Paulay, T., & Priestley, M. J. N. (1992). Seismic design of reinforced concrete and masonry buildings. Wiley. https://doi.org/10.1002/9780470172841

Raykov, S. (2015). Investigation of the behavior of exposed steel column bases when resisting shear forces through anchor bolts (Doctoral dissertation, University of Architecture, Civil Engineering and Geodesy). University of Architecture, Civil Engineering and Geodesy Digital Library. https://eclipse.uacg.bg/catalog/view/GEY8C9DAZQ

Raykov, S., Ganchev, O., Danailov, D., Doykov, I., & Rangelov, N. (2014). Eksperimentalno izsledvane na stomaneni kolonni basi v realni razmeri [Experimental study of steel column bases in real dimensions]. Godishnik na Universiteta po Arhitektura, Stroitelstvo i Geodeziya, 46, 141-154. https://eclipse.uacg.bg/catalog/view/NG4X7HLN6G

Seismosoft. (2024). SeismoSignal [Computer software]. https://www.seismosoft.com

Tapia-Hernández, E., Geneş, M. C., & Gülkan, P. (2025). Damage assessment and seismic response of steel buildings during the Kahramanmaraş, Türkiye earthquakes of February 6, 2023. Earthquake Spectra, 41, 1565-1588. https://doi.org/10.1177/87552930241297937

Thanopoulos, P., Bampatsikos, M. V., Vayas, I., Dinu, F., & Neagu, C. (2024). Earthquake sequence in Kahramanmaraş, Türkiye - Report on the behaviour of precast industrial buildings and proposals for improvement. In F. M. Mazzolani, V. Piluso, E. Nastri, & A. Formisano (Eds.), Proceedings of the 11th International Conference on the Behaviour of Steel Structures in Seismic Areas (STESSA 2024) (Lecture Notes in Civil Engineering, Vol. 520). Springer. https://doi.org/10.1007/978-3-031-62888-7_51

TRIADA-BG. (n.d.-a). Distillery for processing of oil-essential raw materials, Medovo village [Photograph]. https://www.triada-bg.com/tsken.html

TRIADA-BG. (n.d.-b). Rehabilitation, repair and modernisation of Kapitan Andreevo border checkpoint sheds [Photograph]. https://www.triada-bg.com/tsken.html

Yuzbasi, J. (2024). Post-earthquake damage assessment: Field observations and recent developments with recommendations from the Kahramanmaraş earthquakes in Türkiye on February 6th, 2023 (Pazarcık M7.8 and Elbistan M7.6). Journal of Earthquake Engineering, 29, 3367-3392. https://doi.org/10.1080/13632469.2024.2353864

About the authors

TZVETAN GEORGIEV

Associate Professor
Faculty of Structural Engineering
Department: Steel, Timber, and Plastic Structures

Deputy Head of the National Earthquake Engineering Center
University of Architecture, Civil Engineering and Geodesy (UACEG)

Main research area
Steel structures response under seismic actions, Bolts and bolted connections, Low-cycle and extremely low-cycle fatigue, Concentrically Braced Frames (CBFs)

Address
1 H. Smirnenski Blvd., Sofia 1046
E-mail: cvgeorgiev_fce@uacg.bg

This article is an Open Access article distributed under the terms and conditions of the Creative Commons Attribution 4.0 (CC BY 4.0) License (http://creativecommons.org/licenses/by/4.0/).